KSME Journal, Vol. 10, No. 4, pp. 443~449, 1996

A Global Collision-Free Path Planning Using Parametric Parabola Through Geometry Mapping of Obstacles in Robot Work Space

Ihn Namgung*

(Received March 11, 1996)

In this paper, a new algorithm for palnning collision-free path connecting from start to target point is developed using Bézier curve of order two. The control point, i. e. the mid-point of quadratic Bézier curve, determines the shape of parabola and constitutes the Control Point Space. Interference check between path and obstacles creates image in Control Point Space, and this process is difined a Geometry Mapping. After Geometry Mapping of all obstacles, the clear area of CPS, an area not occupied by obstacle images, identifies collision-free path. The path planning algorithm, heance, transform path planning problem in Euclidian Space to point selection problem in CPS. The calculations involved in the algorithm do not require iterative procedures and all the formulas of the solution are derived in closed form. A CPS completely filled with obstacle images indicates that path planning based on parabola is not possible and requires higher order curve with more than one control point.

Key Words: Robot Path Planning, Geometry Mapping, Robot Task Planning, Collision Avoidance

1. Introduction

The use of parametric curve for path planning was introduced previously (Namgung, 1989), in which a collision free path was found in a CPS (Control Point Space) generated by a control point where two line segments meets. The shape of path is then depend on the location of connection points, hence it is called a control point. The control point was organized in a coordinate which defines CPS. The obstacle interference check produced images of obstacles in CPS and this process of transforming obstacles in Euclidian Space into images in CPS is defined to be GM(Geometry Mapping). In this paper, parametric quadratic curve, more specifically a parabola, is used as a base curve for GM. The dimension of CPS is depend on the number of control points and the dimension of base curve. A path planning using higher order curve requires multiple number of control points which leads to a higher dimensional space of CPS, and GM requires numerical calculation consequently it cannot be handled easily.

A parametric quadratic curve can be defined by three vertices and is on a two-dimension. One form of parametric quadratic curve is given by Bézier curve of order two, which was utilized in this paper. This particular curve greatly simplifies GM in calculating the intrference between path and obstacles. Bézier(1972) extended the idea of approximation of a function to approximation of a polygon, in which n+1 vertices of a polygon are approximated via the Bernstein basis. It is also called a Bernstein-Bézier polynomial curve. Bézier curve of order two is a parabola and it approximates a triangle formed gy three vertices, see Fig. 1.

$$R(S) = (1-s)^2 R_0 + 2s(1-s)R_1 + s^2 R_2 = (R_0 - 2R_1 + R_2)s^2 + 2(R_1 - R_0)s + R_0 \quad (1)$$

The valid interval of the parameter s is $0 \leq s \leq 1$ where $s=0$ corresponds to poiht R_0 and $s=1$

* Mechanical Systems Engineering Korea Atomic Energy Research Institute P. O. BOX 105, Yusong Taejon, 305-600

corresponds to point R_2. One should note that in Fig. 1 the lines R_0R_1 and R_1R_2 are tangents to the curve at points R_0 and R_2 respecitively. The location of vertex R_1 detemines the shape of the parabola. The parametric parabola derived above has special meaning in developing collision-free paths in which R_0, R_2 and R_1 are viewed as start point(S), target point(T) and control point (Q), Fig. 1.

2. Work Space Determination for Parabolic Control Point Space

In this sectioin, the formulation of a parametric parabola including the method for setting the ranges of parameters is explained. In Fig. 2 AWS(Actual Woirk Space) is defined to be the actual robot work space bounded by vertices w_1, w_e, w_3, and w_4 and QWS(Quadratic Work Space) is a hypothetical work space defined to enclose AWS. It is so name since the generating curve of QWS is quadratic curve. The size of QWS does not matter as long as it contains AWS. It is important to note the sole purpose for getting QWS is to define a uniform range of parameter ρ, namely 0 to 1(or ρ_{max}), regardless of angle θ. Once QWS is obtained, the outside of AWS should be regarded as obstacle in order to prevent paths passing through AWS.

The defining vertices of quadratic curve is specified by a start point, S, and a target point, T, a center point c, a mid point of ST and remaining vertex Q which controls the shape of curve. The points S, T and Q form a triangle and R(s) is a collision free path connecting points S and T.

$$R(s)=(S-2Q+T)s^2+2(Q-S)s+S \qquad (2)$$

The location of Q is defined by two parameters, θ and ρ in polar coordinate. The parameter ρ defines a bundle of parabolas along the line CQ_{max} and the parameter θ defines families of parabola in angular direction. The curve R(s)* is a Bézier curve defined by triangle SQ_{max} T and passes the boundary of the work space QWS. The range of θ spans from 0° to 360° and the range of ρvaries from 0 to ρ_{max}. The unknown parameter range ρ_{max} can be obtained from QWS.

This sectioin addresses the method of finding the point Q_{max} which defines the largest parabola within the work space, QWS. When control point coincides with centre point parabola degenerates to line ST, accoringly $\rho=0$. The QWS shown by circle in Fig. 2 encloses all of defining vertices of AWS where point W_3 is farthest away from centre point C and it defines the smallest QWS. Exact calculation of ρ_{max} of parabola, R_{max}, is time consuming since R_{max} and the circle is just in contact (both equations are in second order). Here an approximation of QWS indicated as QWS* is used instead. Note from Eq. (1) when s

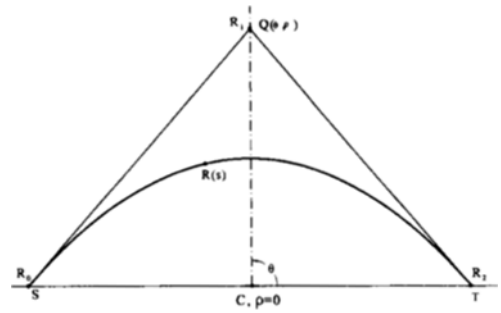

Fig. 1 Parametric representation of parabola(Bézier curve of order two)

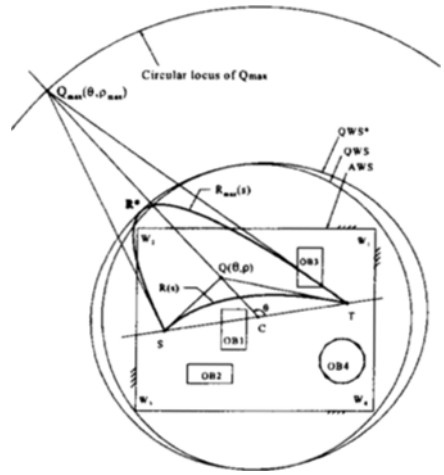

Fig. 2 Construction of Quadratic Work Space and bundle of parabolas

=0.5, the parabola pass through bisection point of line segment CQ_{max} denoted by R*. In other word Q_{max} can be obtained from R* of QWS. This approximation creates QWS* that is slightly larger than circular QWS, see Fig. 2. The circular boundary QWS defined by R* should contain AWS boundary vertices. This is in fact finding the largest distance from centre point to AWS boundary vertices, for example W_3 of Fig. 2. Q_{max} can be obtained using Eq. (2) with s=0.5 and R=R*.

$$Q_{max}-C=2(R^*-C) \tag{3}$$

where C=(S+T)/2. Equation (2) indicates that the radius of circle traced by Q_{max} is twice the radius of circle generated by R*.

So far extreme radius of QWS is discussed. Having calculated $|Q_{max}-C|$, the origin of local coordinate system can be set at C and location of Q_{max} depending on the value of θ can be computed as follows.

$$\begin{aligned} Q_{max,x} &= \frac{|Q_{max}-C|}{|T-S|}\{(T_x-S_x)\cos\theta-(T_y-S_y)\sin\theta\}+C_x \\ Q_{max,y} &= \frac{|Q_{max}-C|}{|T-S|}\{(T_y-S_y)\cos\theta-(T_x-S_x)\sin\theta\}+C_y \end{aligned} \tag{4}$$

Now that the locatioin of Q_{max} can be determined for a given value of θ, the bundle of parabola can be set along the line CQ_{max}.

$$Q=(Q_{max}-C)\rho+C \tag{5}$$

Equation (5) can be substitute into Eq. (2) and get parabolic locus defined by parameters s and ρ.

$$R(\rho,s)=2(C-Q_{max})\rho s^2+2(Q_{max}-C)\rho s+(T-S)s+S \tag{6}$$

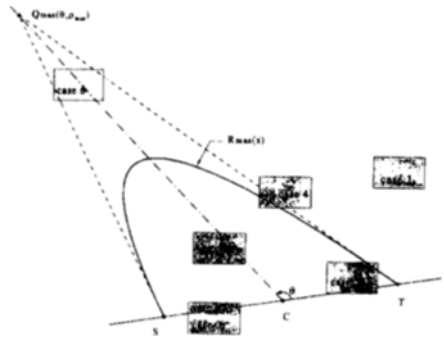

Fig. 3 Classification of obstacles relative to triangle $SQ_{max}T$

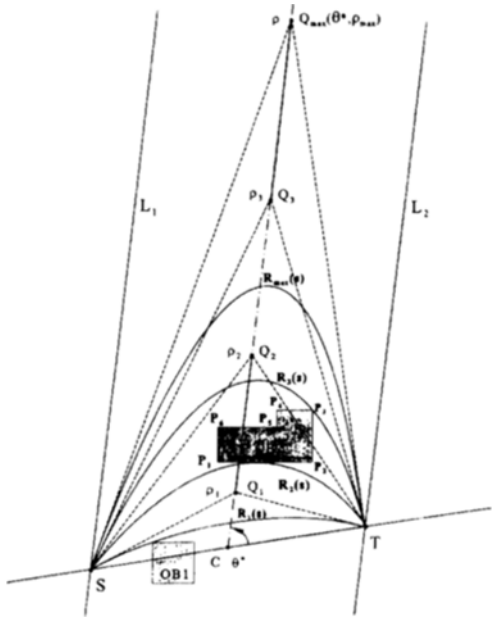

Fig. 4 Interference between a bundle of parabola and obstacles

3. Intersection of Parabolas with an Obstacle

3.1 Categorization of obstacles

Obstacle interference of a bundle of parabolas for a given value of θ is presented in the next section. Actual calculation of obstacle interference can be delayed until categorization of obstacle is done. Figure 3 shows classificatioin of obstacles relative to the triangle $SQ_{max}T$. The reason for doing this is to reduce the calculations involved in interference check which is much more complicated than categorization presented below.

From Fig. 3, number of cases can be observed as follows.

i) Case 1, obstacle is located completely outside of triangle $SQ_{max}T$, no interference check is neces-

say.

ii) Case 2, obstacle is located completely inside of triangle $SQ_{max}T$, may return two clear ranges of ρ.

iii) Case 3, obstacle intersects line segment ST, lower bound of clear range of ρ is obtained.

iv) Case 4, obstacle intersect line segment Q_{max} T or Q_{max} S, upper bound of clear range of ρ is obtained.

v) Case 5, obstacle intersect both line segment ST and Q_{max} T or Q_{max}S, no interference check is necessary. Bundle of parabolas are completely blocked by the obstacle.

vi) Case 6, obstacle intersect both line segment Q_{max}T and Q_{max}S, obstacle may be located outside of parabola.

The categorization can be done using line intersection between traingle $SQ_{max}T$ and obstacle edges.

3.2 Interference of obstacles and parabola

Figure 4 shows obstacle and a boundle of parabolas. It is clear that the obstacle limits the valid range of parameter ρ. The maximum range of blocked value of parmeter of ρ due to interference check with an obstacle requires two different kind of interference calculation. One is a contact between path and a vertex of the obstacle and the other is a contact between path and an edge of the obstacle. For instance, OB2 in Fig. 4, vertex P_3 is in contact with parabola $R_3(s)$, and edge P_1P_2 is in contact with parabola R2(s). Because parameter ρ_2 generates $R_2(s)$ and ρ_3 generates $R_3(s)$, the issue is how to calculate ρ_2, and ρ_3. Additionally it has to be decided among which of the intervals $0\leq\rho\leq\rho_2$, $\rho_2\leq\rho\leq\rho_3$ and $\rho_3\leq\rho\leq 1$ parabolas intersect the obstacle. The categorizatioin described in previous section is used to determine the interval in which actual interference occurs.

The contact between a vertex of obstacle and a parabola can be checked by substituting vertex point, P, into the left hand side of Eq. (6). Eliminate parameter ρ and solve for s.

$$s=\frac{(C_y-Q_{max,y})(P_x-S_x)-(C_x-Q_{max,x})(P_y-S_y)}{(C_y-Q_{max,y})(T_x-S_x)-(C_x-Q_{max,x})(T_y-S_y)} \tag{7}$$

Parameter s represents a point along the parabola. Parameter ρ is obtained by substituting (7) into (6) provided that the denominator of Eq. (7) does not vanish.

$$\rho=\frac{(P-S)-(T-S)s}{2s(1-s)(Q_{max}-C)} \tag{8}$$

The parameter ρ can be calculated by substituting either x or y coordinate values and result of (7). If both the solutions of s and ρ are withing $0\leq s\leq 1$ and $0\leq\rho\leq 1$, contact between vertex P and parabola R(s) occurs. The contact between an obstacle edge and a parabola can be checked by equating equation for edge of obstacle, for example P_iP_j, and parabola given by Eq.(6).

$$\begin{aligned}(P_j-P_i)t+P_i=&2(C-Q_{max})\rho s^2\\&+2(Q_{max}-C)\rho s\\&+(T-S)s+S\end{aligned} \tag{9}$$

Parameter t can be eliminated from Eq. (9).

$$A\rho s^2+(-A\rho+B)s+C=0 \tag{10}$$

where $A=2(Q_{max,x}-C_x)(P_{j,y}-P_{i,y})-2(Q_{max,y}-C_y)(P_{j,x}-P_{i,x})$

$B=(T_y-S_y)(P_{j,x}-P_{i,x})-(T_x-S_x)(P_{j,y}-P_{i,y})$

$C=(S_y-P_{i,y})(P_{j,x}-P_{i,x})-(S_x-P_{i,x})(P_{j,y}-P_{i,y})$

Equation (10) has double roots in s, because the parabola is just in contact with the edge of the obstacle defined by P_i and P_j. Thus the discriminant of Eq. (10) will vanish:

$$A^2\rho^2-2A(B+2C)\rho+B^2=0 \tag{11}$$

Equation (11) may have two different solutions for ρ as shown in Fig. 5 in which R_1 and R_2 are the corresponding curves.

$$\rho=\frac{B+2C\pm 2\sqrt{(B+C)C}}{A} \tag{12}$$

Figure 5 revelals that the root with bigger value is the possible valid solution due to the fact that the parameter value s at contact point for smaller

value of ρ is always outside the range. The corresponding double root s can be obtained by substituting bigger value of ρ into Eq. (10).

$$s=\frac{C\pm\sqrt{(B+C)C}}{B+2C\pm2\sqrt{(B+C)C}} \tag{13}$$

where A, B and C are defined in Eq. (10). The parameter t can now be calculated from Eq. (9) provided that the denominator does not vanish. If the values of ρ, s and t are all within zero and one, a contact occurs. If edge of obstacle is parallel to the line CQ, the denominator of Eq. (12) vanishes and ρ becomes infinite.

When considering a contact of a vertex or an edge with parabolas, singular cases associated with the values of ρ and s, such as $s=0$, $s=\infty$ and ρ or s being indeterminate may arise. If an edge of an obstacle under consideration lies on the line ST, coefficients B and C vanish from Eq. (10), thus ρ becomes zero from Eq. (12) and s becomes indeterminate from Eq. (13). If an edge under consideratin is parallel to CQ, the coefficient A vanishes from Eq. (10). A simple and general method to avoid this situation to compare the denominator with the numerator of Eq. (12) beform evaluating division. If the numerator is less than the denominator, ρ is in the range $-1<\rho<1$ and the division should be evaluated, otherwise the evaluation can be skipped. Finally if the discrimant of Eq. (10) is greater than zero, a negative value of $(B+C)C$ freom Eq. (13) results. This case produces an imaginary value of ρ from Eq. (13). This case arises when an edge under consideration is located within two lines indicated by L_1 and L_2 and extension of the edge intersects line segment ST. Such cases can be avoided by computing the discriminant of Eq. (10). A negative value of discriminant indicate no further evaluation is necessary and intersection check need vertex contact given by Eqs. (7) and (8).

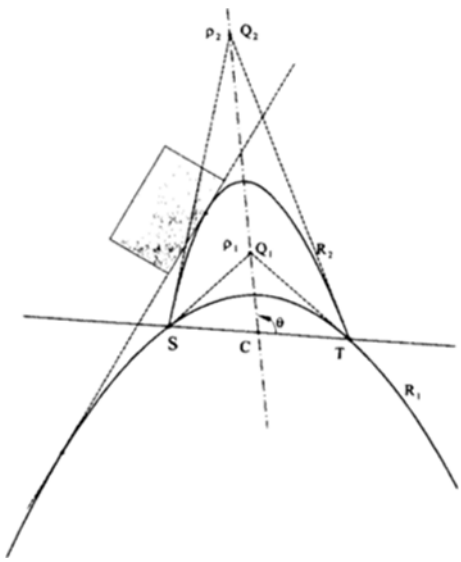

Fig. 5 Two possible cases of contact between a line and parabola

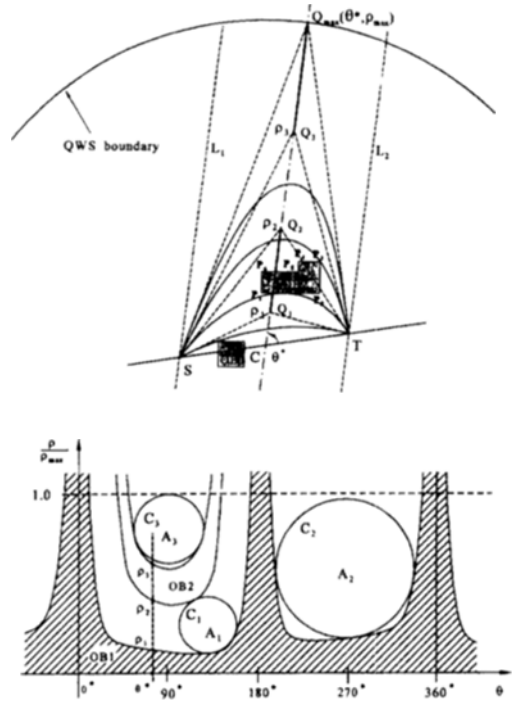

Fig. 6 Geometry Mapping of obstacles from Euclidian Space into parabolic CPS

3.3 Combined blocked range of parameter for construction of obstacle image in CPS

Since the calulation of the intersection between an obstacle and bundle of parabola produces

blocked range of parameter ρ, the final blocked range of ρ is union of all blocked ranges of ρ. Figure 6 shows GM produced by the intersection of parabolas with two obstacles, where θ^* indicates the rotation angle defining the family of parabola. The ranges of ρ in which parabolas interfere with obstacle OB1 and OB2 are $0 \le \rho \le \rho_1$ and $\rho_2 \le \rho \le \rho_3$. Thus the clear range of ρ is $\rho_1 \le \rho \le \rho_2$ and $\rho_3 \le \rho \le 1$, where ρ_{max} is set to 1. In Fig. 6, the dashed line corresponds to θ^* and values of ρ_1, ρ_2 and ρ_3 are plotted accordingly. To create whole images of obstacles in parameter space, ranges of ρ for different values of θ have to be calculated. Such a precess creates images in parabolic CPS as shown in Fig. 6.

The Geometry Mapping developed above finds obstacle interfering ranges of ρ for a given value of θ, hence the mapping is discrete in parameter θ and exact in ρ for that particular value of θ. One should note that geometric mapping for the entire range of θ is not necessary because the values of θ near 0° and 180° produce sharp parabolas and passes near by line segment ST. Any point from the clear area of parameter space corresponds to a collision-free parabolic path. It is apparent that selecting a point that is farthest away from boundaries of all obstacle images gives the safest path. The ranges of ρ for each different value of θ are compared to determine the widest range of ρ, and the mid value of that range is selected as the value of ρ. This pair is only an approximation of the safest path, since the comparision is made in θ-direction only. The true safest path can be obtained from the largest inscribing circle of clear area. Figure 6 shown circles C_1 and C_2, one for upside of line ST and the other form down side of line St. The circles C_1 and C_2 are largest one inscribing clear area A_1 and A_2. Hence the center point of circles C_1 and C_2 anre the safest collision-free path.

Search for the safest path may not be necessary because any point in the clear area of the parameter space is already a collision-free parabolic path. It is also possible to select the shortest path in terms of parabolic path by searching for a point from clear area of parabolic CPS. An approximation for the shortest path is finding the smallest value of ρ from clear areas of CPS. In essence geometric mapping converts the problem of selecting a path in Euclidean space to the problem of selecting a point in parameter space, which is obviously an easier problem.

The Geometry Mapping presented so far is 2D case, however, the algorithm can be applied to 3D case. Note that a quadratic curve is defined by 3 vertices (S, T, and Q), and a plane can be defined by non-collinear 3 vertices. To define a 3D quadratic curve, an additional parameter is required (say ϕ) to define the skew angle of plane that contains S, T, and Q. The parameters ϕ, ρ, and θ are used to define position of Q and the plane. This plane can be treated as a cutting plane of obstacles and the images on the cutting plane are used for 2D Geometry Mapping. This process reduces 3D obstacle into 2D obstacle.

4. Conclusions and Discussions

Path planning based on parametric parabola is introduced in which obstacles in Euclidean Space are mapped into images in Control Point Space. A parametric parabola represented by Bézier curve is used in the development of algorthm in which end points of parabola correspond to the start and target points. The mid-point of parabola controls the shape of path. The algorthm maps obstacle in Euclidean Space into images in parabolic CPS, which is defined to be a Geometry Mapping, and changes path planning problem in Euclidian Space into point selection problem in parabolic CPS. The algorithm involves no interative calculation in doing GM. All cases including singularity have been identified by geometric relations and all formulas have been derived in closed form. A clear cut determination of success of path planning is indicated by the existence of free space of parabolic CPS. A CPS completely filled with obstacle images indicates that path is not available with parabolic curve and requires higher order curve or increased number of control points.

5. References

Bézier, P., 1972, *Numerical Control-Mathematics and Application,* Translated by Forrest A. R. and Pankhurst, A. F., Wiley John & Sons, New York.

Brooks, R. A., 1983, "Solving the Find-Path Problem by Good Representation of Free Space," *IEEE Trans. on Systems,* Man and Cybernetics, Vol. SMC-13, No. 3, pp. 190~197.

Faux, I. D. and Paratt, M. J., 1979, *Computational Geometry for Design and Manufacture,* John Wiley & Sons, New York.

Khosla, P. and Volpe, R., 1988, "Superquadric Artificial Potential for Obstacle Avoidance and Approach," *IEEE Proc. Int. Conf. on Robotics and Automation,* Philadelphia, pp. 1778~1784.

Lozano-Pérez, T., 1987, "A Simple Motion-Planning Algorithm for General Robot Manipulators," *IEEE J. of Robotics and Automation,* Vol. RA-3, No. 3, pp. 224~238.

Namgung, Ihn, 1989, "Planning Collision-Free Paths with Applications to Robot Manipulators," Ph. D. Dissertation, University of Florida.

Shin, D. H. and Ollero, A., 1995, "Mobile Robot Path Planning for Fine-Grained and Smooth Path Specifications," *Journal of Robotic Systems,* Vol. 12(7), pp. 491~503.

Volpe, R. and Khosla, P., 1987, "Artificial Potentials with Elliptical Isopotential Contours for Obstacle Avoidance," *IEEE Proc. 26th Conf. Decision and Control,* Los Angeles, pp. 180~185.